Remote Autonomous Mapping of Radio Frequency Obstruction Devices

Jorgen Baertsch, Ian Cooke Kennedy Harrmann, Mary Landis, Sarah Larson, Harrison Mast, Ethan Morgan, Selby Stout, Jake Ursetta, Justin Williams, Samantha Williams

UNIVERSITY OF COLORADO, AEROSPACE ENGINEERING SCIENCES

As GPS continues to gain popularity in nearly every aspect of our daily lives, it has also increasingly become a target for radio frequency interference (RFI) and other emerging threats (ET). This paper presents a payload designed to operate on a small scale unmanned aerial system (UAS) to detect and localize RFI and ET sources, while autonomously navigating in a GPS-denied environment. Conventional civilian UASs typically rely on GPS and low-cost inertial sensors, such as an inertial measurement unit (IMU), to provide guidance and navigation solutions. The presence of RFI and ET can potentially degrade the GPS signal-to-noise ratio which impacts the accuracy and availability of the navigation solutions. Some sources generate spoofing signals that contain false satellite ranging or navigation message information, which leads to the calculation of an incorrect receiver location. Under GPS-denied conditions, the autonomous navigation solution presented in this paper is based on an extended Kalman filter (EKF) integration of measurements from a consumer-grade MEMS IMU, a magnetometer, an optical flow sensor, a LIDAR range finder, a pitot tube, and a barometer. For interference source detection and localization, a radio frequency (RF) front end antenna operating at the GPS L1 band is used to sample raw intermediate frequency (IF) signals at 5MHz rate. The automatic gain control (AGC) in the RF front end effectively provides the interference signal power measurements. An onboard communication device transmits the IF samples, AGC measurements, EKF outputs, as well as the onboard GPS receiver measurements to a ground station for post-processing and analysis. The work presented in this paper is the result of a senior capstone project at the Aerospace Engineering Sciences Department at the University of Colorado Boulder. The prototype payload and GNS software are designed to meet the requirement of autonomous navigation in GPS-denied environment within a 500-m radius for up to 2 minutes while maintaining 3D platform localization error of 40-m. The UAS will switch to GPS-based navigation solution in areas where interference signal power is below one standard deviation from standard input. Detailed payload design and flight test results will be presented in this paper

Nomenclature

α	Path Loss Coefficient
λ	Signal wavelength
AGC	Automatic Gain Control
$AHRS$	Attitude and Heading Reference System
D	GPS-denied Area Flight Path Length [m]
d	Distance from source to receiver
EKF	Extended Kalman Filter
ET	Emerging Threat
G_r	Antenna gain of the receiver
G_t	Antenna gain of the transmitter
GPS	Global Positioning System
L	Environment losses
P_{actual}	Actual measured power
P_{kl}	Estimated Power Difference
PPD	Personal Privacy Device
Q	Objective Function
R	Radius of GPS-denied Area
R/r	Sensor Radius Ratio []
RFI	Radio Frequency Interference
UAS	Unmanned Aerial System
x/y	Grid location on search area
x_K/y_L	Known locations on path on UAS path

1. Introduction

The purpose of RAMROD (Remote Autonomous Mapping of Radio Frequency Obstruction Devices) is to design, build, and test a system that can localize an RFI source, affecting the L1 and L2 GPS bands, using an autonomous fixed wing UAS. The major challenge with this project is designing the flight software to work properly in GPS denied conditions while minimizing positional error. This problem can be solved by accurately measuring the AGC, and thus the interference, on the GPS bands to determine when the GPS signal can no longer be trusted. This process is completed using an additional payload containing a modified signal filter that is placed on-board the UAS. When the GPS signal can no longer be trusted, the flight system is then prompted to switch to an inertially guided flight mode that does not rely on GPS for navigation. Minimizing the positional error, defined as under 40m after a 1km linear distance, in this GPS denied state is possible by using an array of sensors including a barometer, magnetometer, 3-axis accelerometers, 3-axis gyroscopes, and optical flow. The positional estimations, created by integrating these measurements through the on-board EKF estimator, along with the AGC power measurements are then required to be downlinked to the ground station, in real time, to be post-processed for localization of the RFI source.

The full mission level Concept of Operations (CONOPS) can be seen in Figure 1. In order to achieve full mission success, the UAS shall fly along a pre-programmed autonomous flight path while carrying all necessary payload hardware to localize an RFI source. During the flight plan the payload will detect an RFI source by registering a change in power on the GPS bands. The flight software must then be prompted to change flight modes within 1 second of detecting the change in power and fly without GPS until the interference from the source is back under the acceptable threshold. During the entire flight plan, the positional data, AGC data, and IF data will be transmitted to the ground over a LTE network connection. After fully completing the flight plan, the UAS will land autonomously and the data will be post-processed to localize the RFI source. This paper serves to outline the theory and design used to measure the strength of the RFI source, how these measurements are used to initiate a change in flight mode, how the positional error is minimized during GPS denied flight, and how this data is down-linked in real time. The methods and current results for verification and validation of these critical project elements will then be presented to prove proper functionality of the system.

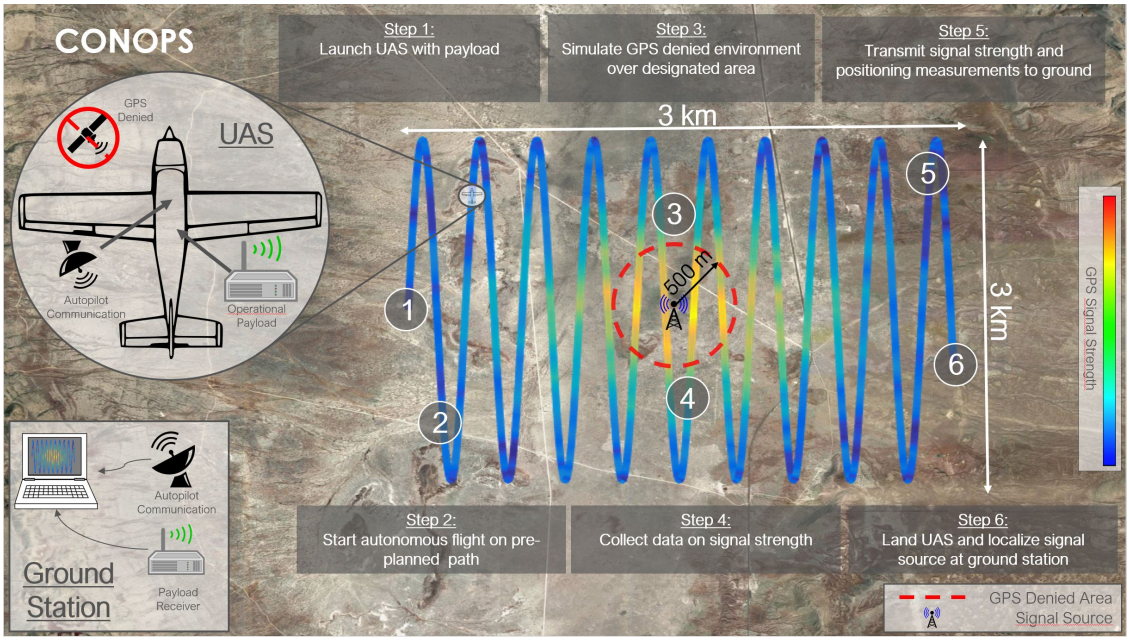

Figure 1: Mission Level CONOPS

2. RFI Localization Theory and Design

2.1. Power Difference of Arrival Localization

The RAMROD system is designed to localize an RF signal using a Power Difference of Arrival (PDOA) method. This method compares the measured signal attenuation between two different points in space to an estimated signal attenuation based on free path loss theory and calculates the most likely location of the interference device. This

method is ideal for the RAMROD system because the payload will measure the signal strength on the GPS band as well as an estimated position based on inertial sensors when the system is within close proximity to a PPD. This data can be used to create an effective map of the GPS denied region over an extrapolated grid, and the location where the signal attenuation most closely matches the estimated path loss will provide the estimated PPD location.

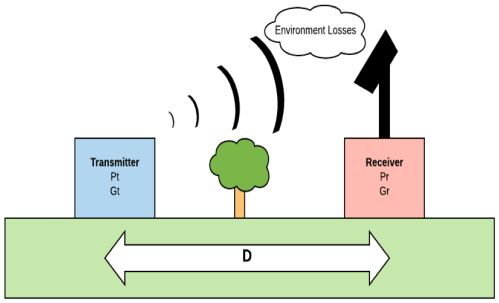

Figure 2: Signal attenuation based on free path loss

The PDOA technique was developed using the algorithmic solution of linear least-squares curve fitting. The path loss coefficient α (shown in Equation 1) can be determined through preliminary environmental testing. The signal attenuation can then be modeled and a predictive power profile of the search area can be developed. After the signal data is obtained during flight, the actual power difference between two points can be compared to the predicted signal attenuation. This prediction is carried out for each data point gathered and is compared to a finite grid of the entire search area. The result is an objective function Q as shown in Equation 4. The function Q is defined for the entire search grid, and the grid coordinates where this function is minimized yield the predicted location of the RFI source.

$$\frac{P_r}{P_t} = G_t G_r \frac{\lambda^2}{(4\pi)^2 D^{-\alpha} L} \tag{1}$$

$$P_{kl} = P_k - P_l = 10\alpha \log_{10}\left(\frac{D_l}{D_k}\right) \tag{2}$$

$$P_{kl} = 5\alpha \log_{10}\left[\frac{(x-x_l)^2 + (y-y_l)^2}{(x-x_k)^2 + (y-y_k)^2}\right]^2 \tag{3}$$

$$Q(x,y) = P_{measured} - 5\alpha \log_{10}\left[\frac{(x-x_l)^2 + (y-y_l)^2}{(x-x_k)^2 + (y-y_k)^2}\right]^2 \tag{4}$$

The RAMROD localization algorithm was tested with sample data that was collected with a similar UAS that measured signal strength on the 2.4GHz WiFi band (to simulate GPS interference) as well as true GPS position data. The results from this test are shown in Figure 3. The emitter position was estimated 29.74m away from the actual emitter location with only 109 data points used. This result provides an important proof of concept for PDOA and a baseline error threshold. Although the RAMROD system will use far more data samples, the drift of the UAS during inertial navigation is expected to produce significant error in localization.

2.2. Automatic Gain Control on L1 and L2 GPS Bands

The payload on-board the UAS measures the signal strength on all GPS bands, stores the data, and downlinks some of this data through a LTE cellular network. As previously mentioned the data collected serves two major purposes: to prompt the flight system to change flight modes when an RFI source is present, and to be used in post-processing to localize that source. An antenna, located on the underbelly of the aircraft, measures the power level on four channels in two GPS bands and collects Intermediate Frequency (IF) and Automatic Gain Control (AGC) data. The AGC data will be used on the ground station to create a power profile with the PDOA localization algorithm described above.

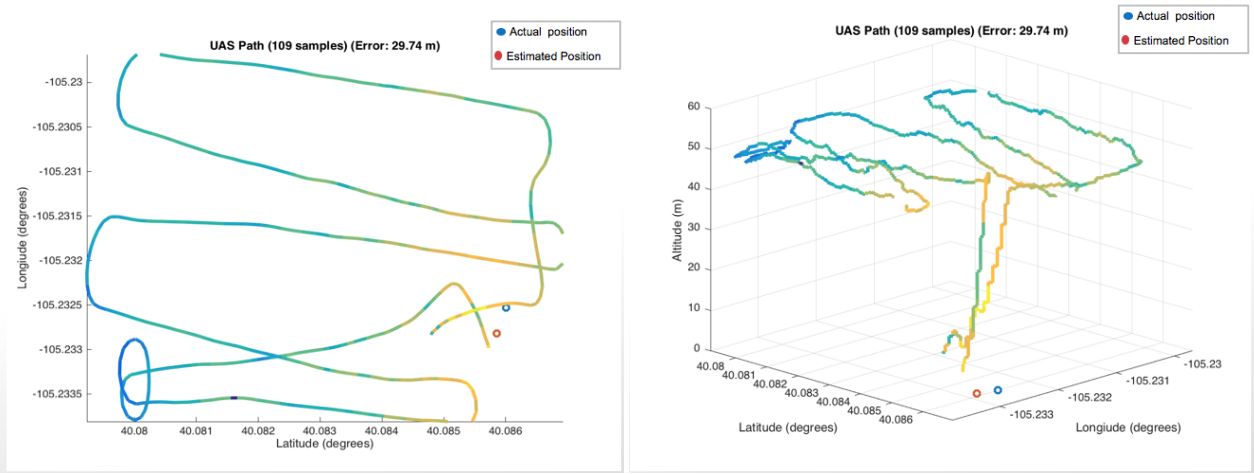

Figure 3: Localization Model: 2D (left) and 3D (right)

The IF data is collected to be later used for a more accurate localization method that utilizes a time difference of arrival (TDOA) algorithm. This is outside the scope of this project and therefore will not be discussed past the point of data collection and transmission. The data collected is then pushed through a signal filter to smooth out any unwanted noise. This filtered data is then sent to a microprocessor located within the payload which is used to store the data on an on-board storage device and push the data through the LTE connection to the ground station.

Figure 4 shows sample AGC data, on both the L1 and L2 bands, taken over a 250s time period. The data has the ability to be stored in 19 different bins to quantify the power measurement at any given time. This data is under nominal conditions, with no interference present, which is why the values remain relatively constant over the entire time period. If there was a PPD in the area, the AGC value would decrease. This can be seen in Figure 5, which shows how the AGC level drops as the UAS moves closer to the RFI source. This extreme change, quantified as two standard deviations below the norm, is used to trigger the change in flight mode within the flight software.

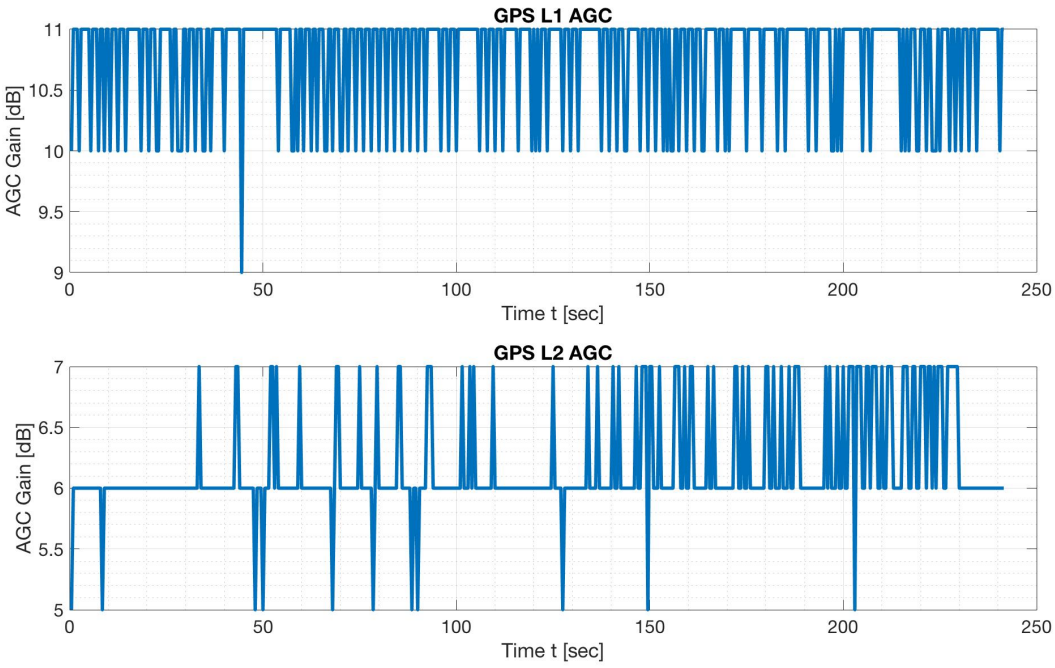

Figure 4: Sample AGC data over a 250s second period.

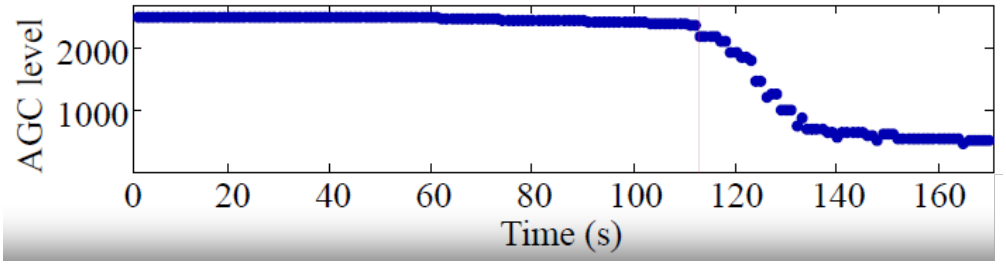

Figure 5: Expected change in AGC data while approaching interference source.

3. GPS Denied Guidance

Throughout the initial design of this project, numerous methods were considered that would allow the UAS to safely navigate a GPS denied environment. Among these were concepts such as LTE Localization, Simultaneous Localization and Mapping, and a solely optical based localization method. However, most of these would require the addition of numerous instruments, and would require heavy modification to the existing flight software. For that reason, a system relying on a reliable Inertial Measurement Unit (IMU) accompanied by various other sensors (Optical flow, magnetometer, barometer) was chosen as the method of GPS denied guidance for the UAS.

3.1. Inertially Guided Flight Using an Extended Kalman Filter

As mentioned, the primary reason for utilizing an INS is the existing support within the ArduPilot flight software. The PixHawk flight controller comes stock with a full inertial sensor package, including three 3-axis accelerometers and three 3-axis gyroscopes. The data from these sensors is fused using an extended Kalman filter (EKF), which comes as a built in functionality within the ArduPilot flight software.

Non-inertial sensors will provide additional data, or reference measurements, which will be utilized by the EKF to better estimate the error in inertial measurements. This provides a more accurate estimate of the UAS state. Unlike the inertial data, these reference measurements do not require an integration step before they may be incorporated into the state. For example, the acceleration measured by the accelerometer must first be integrated (which introduces an error of its own) before the velocity is known. On the other hand, the pressure differential read by an airspeed sensor is directly proportional to the airspeed experienced by the UAS. The other instruments that feed reference data into the filter are two barometers (pressure measurement proportional to altitude), three 3-axis magnetometers (giving a magnetic heading), an optical flow sensor (reading change in relative position), and a LiDAR range finder (measuring distance above ground level). GPS is typically the most trusted reference measurement, however, when going GPS denied, this will not be an option. Once in the GPS denied mode, data from an optical flow sensor, paired with a LiDAR range finder, will be passed to the filter as a reference measurement. The optical flow sensor captures images at 400 Hz, and by knowing its current altitude, is able to calculate a change in position from one image to the next by comparing how objects have moved in one image relative to the previous. The EKF will take in data from these inertial and reference sensors, apply an appropriate gain to each, use the previously estimated state as an initial condition, and fuse this with knowledge of the dynamics of the physical system to arrive at a newly estimated state and estimated error. The estimated error is incorporated into the filter during the next step so that the resulting estimate accounts for inertial measurement error due to sensor offsets, drifts, and biases.

3.2. Propagation of Positional Error

While the PixHawk flight controller comes with 3 accelerometers and gyros, the accuracy of these are limited such that GPS is necessary to continuously calibrate throughout flight. For this reason, it was necessary to incorporate an additional IMU designed with more accuracy and stability. A requirement of this project is to localize RFI and ET sources within 40 meters, as such, a requirement of the state estimate is that the positional error must stay below 40 m after 200 seconds without GPS. The 200 seconds is derived from a ground speed of 10 m/s, and a maximum GPS denied linear distance of 2 km. In order to prove this feasibility, static testing with the improved IMU was conducted. The accelerations in each direction were twice integrated to provide position, and if this position is below 40 m, then it is assumed that the error can only be reduced with the addition of the EKF and reference measurements. Figure 6 shows the integrated x, y, and z position over 200 seconds, and Figure 7 shows the total positional error summed in quadrature.

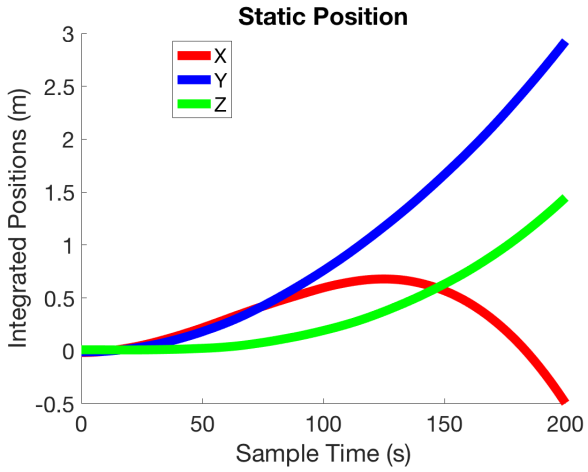

Figure 6: Static position measured by IMU

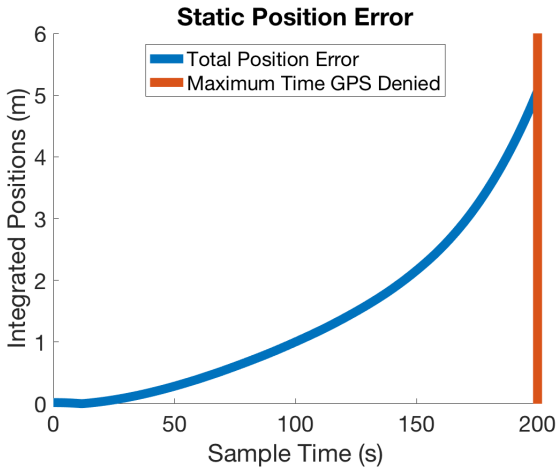

Figure 7: Static 3D positional error from IMU

It can be seen in Figure 7 that after 200 seconds there is only about 5 meters of error. It can also be seen that this error grows in an exponential manner, which is why the EKF and additional measurements are necessary. This error will be further reduced when the error in the z direction is nearly eliminated by a barometer.

4. Payload and Flight Systems Interface

4.1. Flight Mode Switch

As explained in Section 2.2, the AGC feedback data is measured on the GPS bands on the NT1065 signal filter, which is then sent to the MicroZed microntroller. Performing characterization tests with the antenna in different scenarios (far away from noise sources, around various noise sources) yields an expected noise floor. When recording AGC data in GPS-denied environments, once the AGC value exceeds a 2σ deviation from the norm on any GPS band, it is determined that the UAS is operating in the presence of an RFI emitter. The AGC signal is continually sent to the PixHawk flight controller over a serial connector at a rate of at least 3Hz, sending a 5-bit number indicating whether the AGC data is above or below this 2σ threshold. Only one byte is necessary to send the AGC data since the AGC data only holds 19 possible values.

When the PixHawk receives an AGC value greater than 2σ, representing entering the sphere-of-influence of a PPD, the Pixhawk cuts the GPS input to the Kalman filter and allows the optical flow measurements to be fused into the filter. The flight controller then continues navigating to the next waypoint using its inertial sensors until the AGC data falls below the threshold and is out of the sphere-of-influence. Once this occurs, the GPS data input to the Kalman filter is restored and the optical flow input is removed. The Kalman filter then experiences innovations representing the

difference between estimated measurements and GPS truth measurements, for each of its 24 states. These innovations are corrected by the autopilot's Attitude and Heading Reference System (AHRS), adjusting for the filter's divergence due to lack of absolute measurements of position from the GPS.

In return, the PixHawk sends its timestamped estimated and true position measurements to the MicroZed, via a UART connection, at the same 3Hz. These measurements include latitude, longitude, and altitude of the aircraft. This data is downlinked by the payload, via the LTE connection, for use in post-processing and localization.

4.2. Downlinking of Data

Figure 8 depicts the interfacing between the various devices associated with processing and downlinking data.

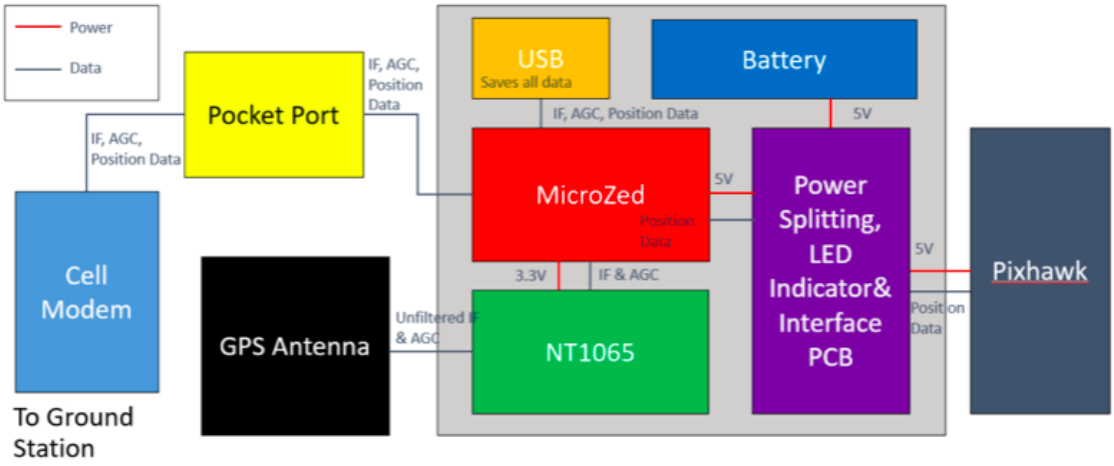

Figure 8: Payload Data Transmission.

All data is downlinked from the payload's microprocessor, the MicroZed. As described in Sections 2.2 and 4.1, it is required to downlink AGC data, positional data, and IF data. Because the IF data is so large, the data is being stored at about 1GB/min, which can be easily stored on an on-board USB Drive. It is expected, based on typical data rates, that the LTE modem can downlink 8-10Mbps, which is not sufficient to downlink all of the IF data. Since the IF data is not required for localization for this project, it was deemed that storing this data was sufficient as long as part of the IF data could be downlinked. It was determined that all positional and AGC data could easily be downlinked with approximately 5% of the downlink capacity, leaving the remaining 95% of the downlinking capacity being open for IF data. The amount of data sent to the ground station via the LTE modem will change depending on the cell coverage available so that it takes less than 10 seconds to send the current set of data. This was accomplished by throttling the amount of IF data being downlinked based on the cell coverage available. If the cell service is poor, the micro-controller will throttle the amount of data being sent to the LTE modem with the goal of always sending the data packet in less than 10 seconds. It is important to note that while the IF data being transmitted might change, all of the positional and AGC data is always downlinked. A visualization of how the down-linking of data will work can be seen in Figure 9.

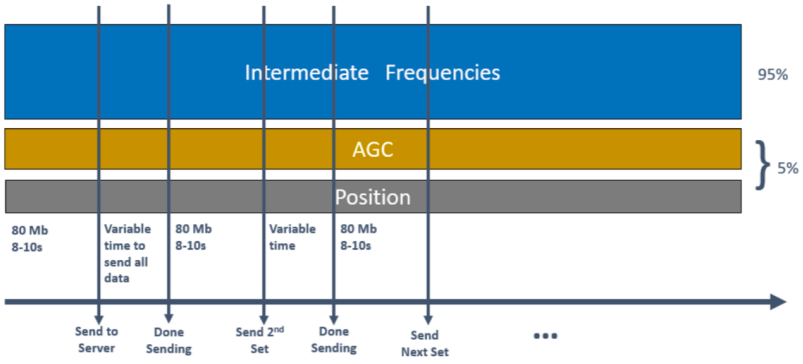

Figure 9: Diagram of the Down-linking of Data.

5. Verification and Validation

The RAMROD system's functionality will be verified through both ground testing and flight testing. Subsystems shall be tested individually before full system integration.

5.1. Ground Testing

The ground testing stage of validation will verify the performance of the payload and software project elements prior to full system integration. Verifying these systems on the ground will maximize the success of the future flight tests and prove the lower levels of success required for mission level testing.

5.1.1. Payload Ground Testing

Beyond basic component functionality testing, there are several ground tests that must be preformed to ensure subsystem success prior to full system testing. The most important of these establish a baseline AGC reading, ensure proper downlinking capacity, verify the interface between the PixHawk and MicroZed, and verify the storage of all data inside the payload.

The AGC data needs to be characterized in order to establish a baseline reading to compare in-flight AGC data to. Initially the antenna will be placed far away from any electronics, GPS, or potential RFI sources to establish baseline AGC data in the presence of no electronics sources. The second portion of this calibration involves placing the antenna onboard the UAS, in the proximity of all of the electronics systems to establish baseline data on board the UAS. Establishing this baseline will ensure less false GPS denied triggers during flight.

Ensuring proper downlinking capacity requires testing in multiple locations with varying cellular coverage. The different locations will include the center of Boulder, CO, where the signal should be the best, and at different rural areas close to the test site where there will be less coverage. The combinations of these tests will show how much data can be sent with different strengths of connections and how that changes the amount of data sent as well as ensure that the system will function as necessary on site. While only a portion of the data will be sent to the ground station, all of the data will be saved to a USB flash drive inside the payload. To ensure that all data can be saved, the system shall be allowed to collect data on the ground for one hour. If the system is working properly then it will save 1 GB per minute of data.

The interface between the PixHawk and the Microzed will be tested on the ground by feeding the MicroZed simulated AGC data. This data will contain a change in AGC power that is representative of a PPD. If the system is functioning properly, the MicroZed will prompt the PixHawk to change flight modes. This can be checked easily with the output logs from the PixHawk. If this final test is successful, along with the tests previously described, then the payload is prepared for full system level testing.

5.1.2. Inertial Navigation Ground Testing

The RAMROD inertial navigation system and flight mode switch functionality shall be tested and verified on the ground before flight testing. The objective is to ensure that the positional error generated by this system is below a 40m threshold. Static testing has verified that the RAMROD hardware baseline drift is below 40m, as shown in section 3.2. In addition to static testing, the full system will be driven a length of at least 2 miles. Halfway through this test a

geographical trigger will be used to switch the flight mode to GPS denied. This not only verifies that the flight mode will switch successfully, but it will also quantify the positional error during the GPS denied period.

5.2. Mission Level Testing

The mission level testing will validate the integration of all RAMROD subsystems. The RAMROD UAS shall fly on an autonomous flight plan over a 3km square search area and gather RF interference data as well as true GPS position data. The RAMROD system will be flown through a GPS denied area 500 meters in radius. Once the RAMROD system detects an increase in GPS signal strength (indicating the presence of a PPD) the autopilot system will switch from a GPS guided flight mode to an inertially guided flight mode. During this time, the inertial navigation system will log position estimates that will be used in the localization algorithm. At least five trials with different PPD locations will be completed to include edge cases where a PPD is located on top of a way point. This is illustrated in Figure 10, where Trial 2 depicts the case where the PPD is located on a way point at the edge of the search area. The target threshold for inertial drift is 40m in any direction, and this will be verified for straight and level flight as well maneuvers in the GPS denied state.

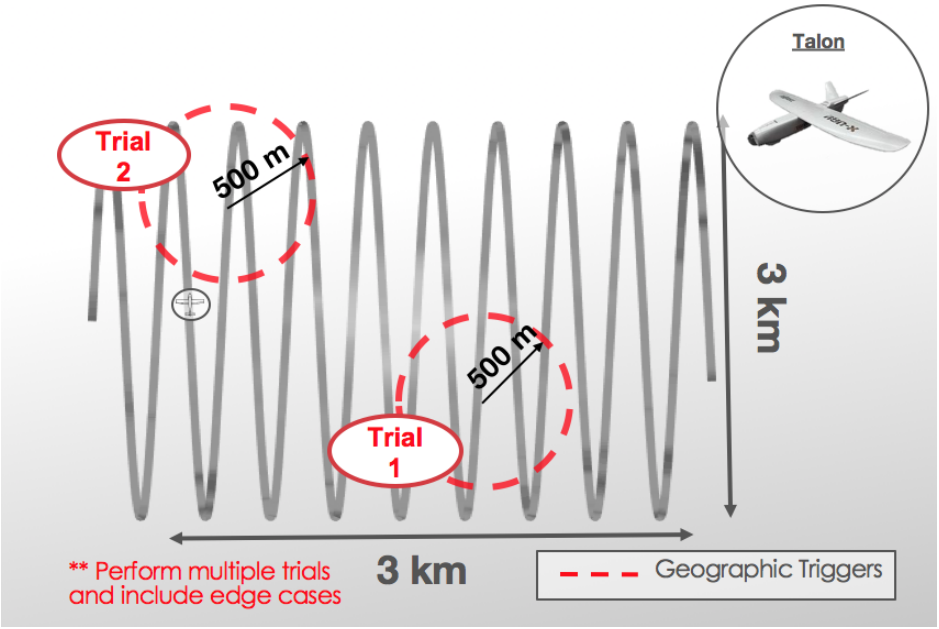

Figure 10: GPS Denied Flight Testing

6. Bibliography

[1] National Coordination Office for Space-Based Positioning, Navigation, and Timing (05 Dec. 2017).GPS Accuracy. Retrieved from https://www.gps.gov/systems/gps/performance/accuracy/

[2] Plane home (10 Dec. 2017). Retrieved from http://ardupilot.org/plane/index.html

[3] Planning a Mission with Waypoints and Events¶. (n.d.). Retrieved December 14, 2017, from http://ardupilot.org/copter/docs/common-planning-a-mission-with-waypoints-and-events.html

[4] Complete Parameter List¶. (n.d.). Retrieved December 14, 2017, from http://ardupilot.org/plane/docs/parameters.html

[5] Extended Kalman Filter Navigation Overview and Tuning¶. (n.d.). Retrieved December 14, 2017, from http://ardupilot.org/dev/docs/extended-kalman-filter.html

[6] MAVProxy¶. (n.d.). Retrieved December 14, 2017, from http://ardupilot.github.io/MAVProxy/html/index.htmlP. (2016, November 02).

[7] Priseborough/InertialNav. Retrieved December 14, 2017, from https://github.com/priseborough/InertialNav

[8] Roll, Pitch and Yaw Controller Tuning¶. (n.d.). Retrieved December 14, 2017, from http://ardupilot.org/plane/docs/roll-pitch-controller-tuning.html

[9] "LIDAR-Lite Rangefinder." LIDAR-Lite Rangefinder — Copter Documentation, ardupilot.org/copter/docs/common-rangefinder-lidarlite.html

[10] "How To Calculate Drag." It's All RC!, 19 Feb. 2014, itsallrc.wordpress.com/2014/02/19/how-to-calculate-drag/

[11] Jackson, B. R., Wang, S., and Inkol, R., "Emitter geolocation estimation using power difference of arrival ," An algorithm comparison for non-cooperative emitters , May 2011.

[12] Chen, H., Lin, T., Kung, H. T., Lin, C., & Gwon, Y. (n.d.). Determining RF Angle of Arrival Using COTS Antenna Arrays: A Field Evaluation [Scholarly project]. In School of Engineering and Applied Sciences Harvard University. Retrieved September 29, 2017

[13] Chen, Y.-H., Lee, W., Lo, S., and Enge, P., "RFI Localization with a 3-Element Beam Steering Antenna," SCPNT Symposium , Nov. 2017.

[14] "Automatic Takeoff." Automatic Takeoff — Plane Documentation, ardupilot.org/plane/docs/automatic-takeoff.html

[15] "Automatic Landing." Automatic Landing — Plane Documentation, ardupilot.org/plane/docs/automatic-landing.html

[16] Morales, J. J., Shamaei, K., Khalife, J., & Kassas, Z. M. (2017, April 03). LTE cellular steers UAV: Signals of opportunity work in challenged environments. Retrieved October 01, 2017, from http://gpsworld.com/lte-cellular-steers-uav-signals-of-opportunity-work-in-challenged-environments/

[17] Thorpe, M., Kottkamp, M., Rössler , A., and Schütz, J., "LTE Location Based Services Technology Introduction" Available: http://www.rohde-schwarz-wireless.com/documents/LTELBSWhitePaper_RohdeSchwarz.pdf

[18] Grade, K., "Introduction to Inertial Navigation and Kalman Filtering," Navigation Laboratory, Jun. 2008.

[19] "A Complete Guide to LiDAR: Light Detection and Ranging," GISGeography Available: http://gisgeography.com/lidar-light-detection-and-ranging/

[20] Bachrach, A., Prentice, S., He, R., and Roy, N., "RANGE - Robust Autonomous Navigation in GPS-denied Environments," Journal of Field Robotics, 2011.

[21] Marcoe, K., “LIDAR an Introduction and Overview.” Portland State University, Fall 2017, http://web.pdx.edu/~jduh/courses/Archive/geog481w07/Students/Marcoe_LiDAR.pdf

[22] Silicon Sensing, ”DMU11-00-0100-132 Rev 3,” DMU11 technical datasheet. 2016.

[23] KVK Industries, ”Guide to Comparing Gyro and IMU Technologies – Micro-Electro-Mechanical Systems and Fiber Optic Gyros.” White paper. 2012.